УДК 551.14:550.3+504.05(477) DOI: https://doi.org/10.24028/gj.v45i1.275130

Native aluminum as indicator of hydrogen degassing in the formation of hydrocarbon fields

O. Lukin[1], *I. Koliabina*[1,2], *V. Shestopalov*[2], *O. Rud*[3], *2023*

[1]Institute of Geological Sciences of the National Academy of Sciences of Ukraine, Kyiv, Ukraine
[2]Radioenvironmental Centre of the National Academy of Sciences of Ukraine, Kyiv, Ukraine
[3]G.V. Kurdyumov Institute for Metal Physics of the National Academy of Sciences of Ukraine, Kyiv, Ukraine
Received 12 January 2023

This work considers the possibility of native aluminum transport with hydrogen fluid, its deposition and preservation in sedimentary rocks, as well as an assessment of the conditions under which this is possible. This problem is currently debatable and is considered in a number of publications. Native aluminum was found in different types of sedimentary rocks of oil-and-gas-bearing basins. So the presence of native aluminum spherulas was established in the dolomites of the Dnipro-Donetsk Basin. By the example of these findings this work shows that the necessary conditions for the formation and long-term preservation of native aluminum are: its migration with the hydrogen flow into the upper layers of the Earth's crust, the creation of temperature and pressure conditions causing water to vaporize, and the formation of a protective film on the surface of the formed native aluminum. The process of native aluminum formation in the sedimentary rocks of oil-and-gas-bearing deposits of the Dnipro-Donetsk Rift described in this work, as well as its findings in other basins indicates the typical character of this process for rift structures of hydrocarbon accumulation. It was assumed, that the oil-and-gas-bearing structure of Dnipro-Donetsk Rift is mantle origin and represents a giant source of deep hydrogen. Some of this hydrogen is consumed to form hydrocarbon accumulations, including known oil and gas deposits, and some of it degasses into the uppermost layers of the Earth's crust. Independent hydrogen fields can also form there, as was the case during the formation of the deposit of geological hydrogen in Mali. It was shown, that the presence of hydrocarbons in the fluids does not affect the processes associated with aluminum. The results obtained indicate significant flows of hydrogen from the mantle to the upper horizons of the Earth's crust. Thus, native aluminum, as well as other native oxyphilic metals in sedimentary rocks of oil-and-gas bearing basins is a search marker of both hydrocarbon accumulations and the important role of deep geological hydrogen in the formation of these accumulations and its possible accumulation in the most reliable traps.

Key words: native aluminium, hydrogen fluides, sedimentary rocks.

Introduction. A scientific sensation arose in the late 1970s and early 1980s when oxyphilic metals, first of all aluminium, were discovered in the reduced form in the native state in various igneous and hydrothermal rocks. Noteworthy, at that time the paper [Oleynikov et al., 1978] on the discovery of native aluminium in the trap rocks of Eastern Siberia suggested that Al^0 formation was caused by the inflow of hydrogen from the lower mantle, creating highly reducing conditions. This process cannot occur in the presence of water in the rocks. In [Novgorodova, 1979, 1983], CO_2 gas was identified as a component preventing the formation of native aluminium, similarly to water. Later, Al^0 was detected in ultrabasic rocks of the Siberian platform [Kovalskiy et al., 1981], in picritic porphyrites of the Gulin-

sky pluton [Oleynikov et al., 1981], in kimberlites of Yakutia [Marshintsev et al., 1981], in hydrothermal ores of the Nikitsky mercury deposit [Kupenko, Osadchy, 1981], in oceanic rocks [Shterenberg, Vasilyeva, 1979; Shterenberg et al., 1986, 1988], in the recent alluvium of the Crimea [Bayrakov et al., 2005], in the low-temperature anomalous formations of the Barakolska depression in the eastern part of Crimea Mountains [Shnyukov et al., 1993], in mud volcano ejecta [Novgorodova, Mamedov, 1996; Shnyukov, Lukin, 2011], at the contact of pegmatites and serpentinized ultrabasic rocks of the Rila Mountains in Bulgaria [Dekov et al., 2009], etc.

A number of publications testify to the fact that molecular hydrogen admixtures are fixed in the composition of natural gas [e.g., Bondarenko et al., 2005; Saranchuk et al., 2008]. In addition, the simultaneous presence of hydrogen and hydrocarbons in gases seeping to the surface has been recorded [e.g., Larin et al., 2015; Nivin, 2016; Prinzhofer et al., 2019]. Therefore, the authors of this work got the idea to use the findings of native aluminum as an indicator of hydrogen degassing activity during the formation of such hydrocarbon deposits.

Native aluminium in oil and gas reservoirs. Findings of native aluminium (NA) in the sedimentary rocks hosting hydrocarbon fields are of considerable interest [Lukin, 2004, 2008]. Native aluminum was found especially in secondary pores of reservoir rocks. The oil fields Lelyakivske and Gnedyshchenske (Dnipro-Donetsk Basin, Ukraine), Kuyumbinske (Eastern Siberia), Talinske (Western Siberia) are confined such reservoir rocks. The actual data on these deposits have been published previously [Lukin, 1997]. In this paper, thermodynamic modeling was performed using data from the Lelyakovskoe field.

The main part of the Ukrainian largest oil pool in the Lelyakivske field is confined to the carbonate reservoir, which is a metasomatically dolomitized Lower Permian reef structure. There, biomorphic limestones were replaced by cavernous porous crystalline-grained dolomites with diverse (pyrite, galena, etc.) sulfide mineralization. Isotope-geochemical data testify to the participation of deep fluids in the processes of secondary dolomitization (Cimmerian phase of tectonic-thermal activation) [Lukin, 1997]. NA is confined there to secondary microcavities (pores, caverns, and cavern fractures). Various deformations of the aluminium inclusions are typical, both syngenetic to their separation (Fig. 1, *a*) and caused by subsequent tectonic stresses and sliding over the diaclase surface (Fig. 1, *b*). In general, they are characterized by the same complex morphology as the NA inclusions in the gabbro-dolerites of traps from the Siberian Platform [Oleynikov et al., 1978] and gold-bearing hydrothermal veins from the Southern Urals [Novgorodova, 1983]. Uneven («corroded») contours (Fig. 1, *c*) testify to the aggressive influence of the alkaline environment (pH of pore solutions in dolomite achieves values of 8—9) at the time when the (micro) inclusions of native Al (an element with sharply pronounced amphoterism) were formed prior to the passivating oxide film formation.In some samples, the presence of NA is registered by X-ray diffraction analysis. Similar to Al^0 from hydrothermal ores [Novgorodova, 1983], the reflex 0.235—0.236 nm is the most intense on the diffractogram of Al-containing secondary oil dolomite from the Lelyakivske field (for Al^0 from gabbro-dolerites and oceanic sediments the strongest line is 0.232 nm).

At the large Gnidyntsivske field, located together with the Lelyakivske field on the southern edge of the Sribnenska Lower Permian saliferous depression in the Dnipro-Donetsk Basin, the reservoir of the massive sheet oil pool is composed mainly of Lower Permian-Upper Carboniferous sandstones (see Fig. 1). Only on the southeastern flank of the Gnidyntsivska brachianticline, the Lower Permian secondary oil dolomites have been recently developed. Similar to the Lelyakivske field, electron microscopic and X-ray analysis showed that these rocks contain NA along with pure native iron, as well as copper, lead, zinc, etc.

Its aggregates with halite, containing grains of iron and other native metals, are of particular interest. According to M.I. Novgorodova

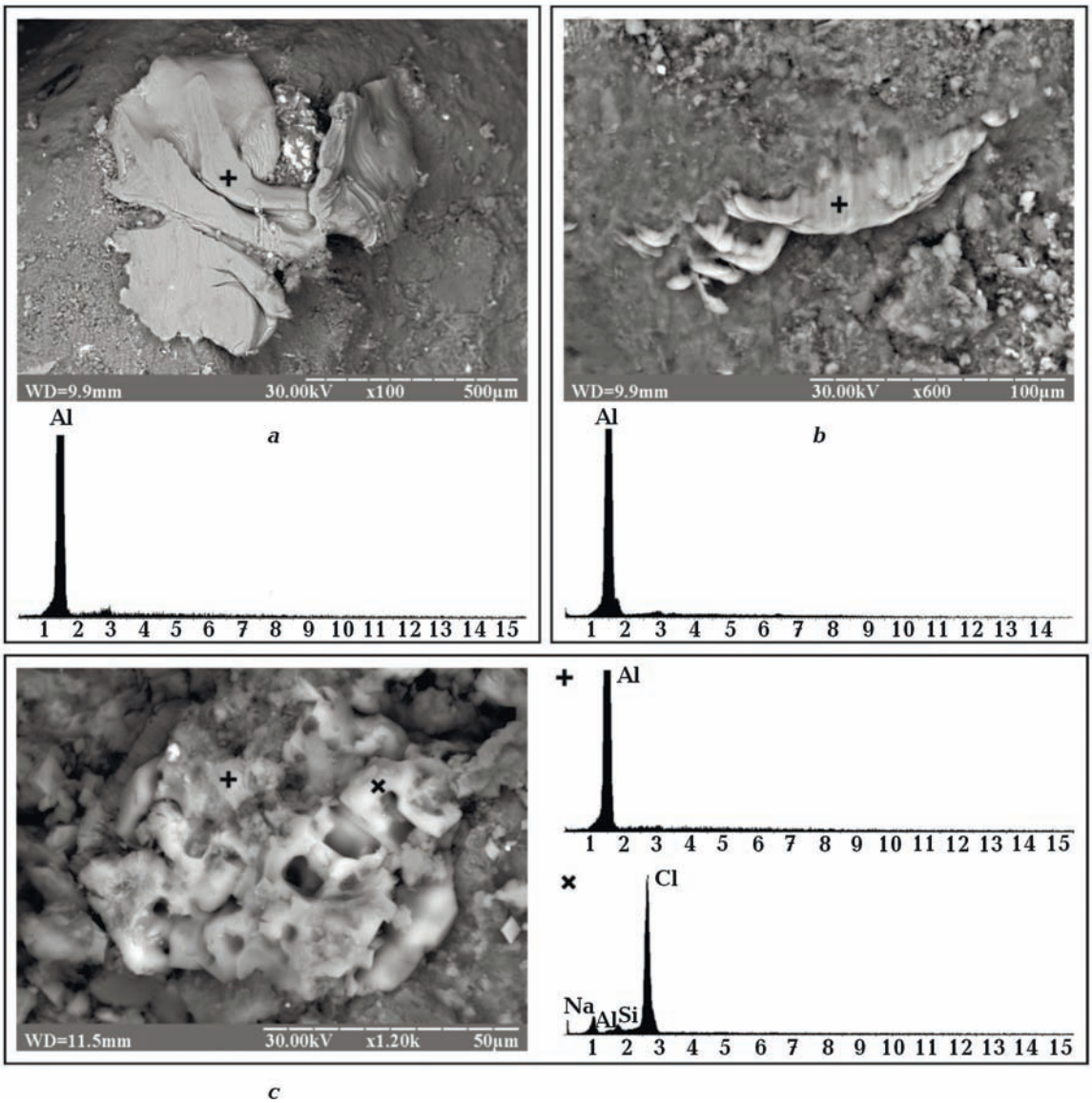

Fig. 1. Native Al in oil dolomites of Lelyakivske (*a*, *b* — well 301, depth 1945.5—1950 m) and Gnidyntsivske (*c* — well 212, depth 1788—1793 m) fields in the Dnipro-Donetsk Basin.

[Novgorodova, 1983], inclusions of halite and sylvin are found practically in all aluminium grains.

Reservoirs of the giant Talinske oil field represent fractured-cavernous-secondary pore metasomatites associated with hypogene-allogenetic transformations of catagenetically-quartzed Lower Jurassic sandy-coarse rocks with reduced primary porosity [Lukin, 1997]. Along with iron, nickel, and zinc, NA inclusions varying in morphology were established inside secondary pores (caverns). In particular, aggregates of its fibrous and lamellar particles were observed (Fig. 2).

Various NA occurrences have been fixed in oil-and-gas fractured-cavernous Riphean dolomites of the giant Kuyumbinske field in Eastern Siberia.

Along with inclusions of laminae and granules, granular-fibrous aggregates (Fig. 3, *a*) and films (Fig. 3, *b*) were also found there.

Despite the stochastic character of the distribution of native-metallic particles and limited observations, the above data allow us to identify oil-and-gas reservoirs as a special type of natural objects containing NA. By

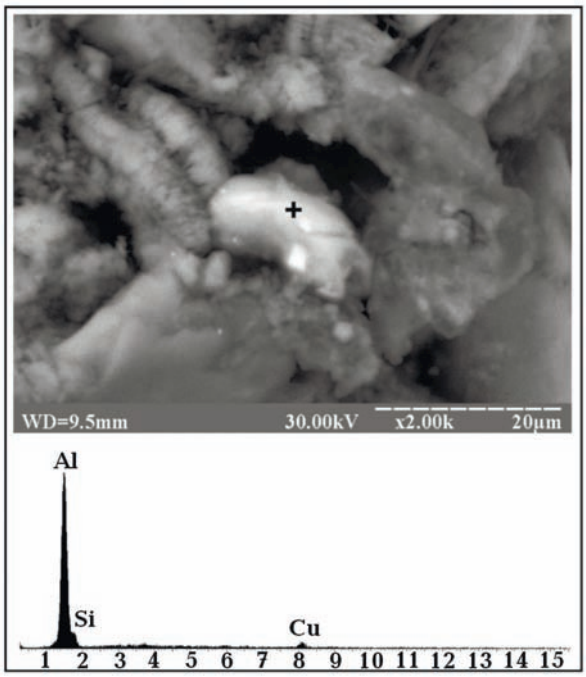

Fig. 2. Native Al in the secondary pore (cavern) of the oil reservoir in the Talinske field (Western Siberia).

chemical composition (Al content over 95 %) and morphological features this is close to NA inclusions in basic magmatic rocks and Au, Hg-bearing hydrothermal veins. Moreover, the above data suggest that its morphological diversity in oil-and-gas reservoirs is much higher. At the same time, it should be noted that the frequency of aluminium occurrence in them is significantly lower as compared to many other native metals.

In this respect, illustrative are the data of studying the inclusions of native metals in the reservoirs of the unique White Tiger oil field (South Vietnamese shelf), whose major massive oil pool is associated with decompacted and metasomatically transformed magmatic rocks. As compared to the other objects studied by the author, these are characterized by the greatest diversity of dispersed particles represented by iron, zinc-copper (natural brass), chromferide, as well as copper, lead, zinc, silver, nickel, chromium, etc. Here, titanium, indium and some previously unknown intermetallic compounds were determined in the native state [Lukin et al., 2007]. Some X-ray patterns, besides native iron, zinc, lead, and zinc-copper, also show lines characteristic of NA. Stochastic character of the distribution of dispersed native metal particles,

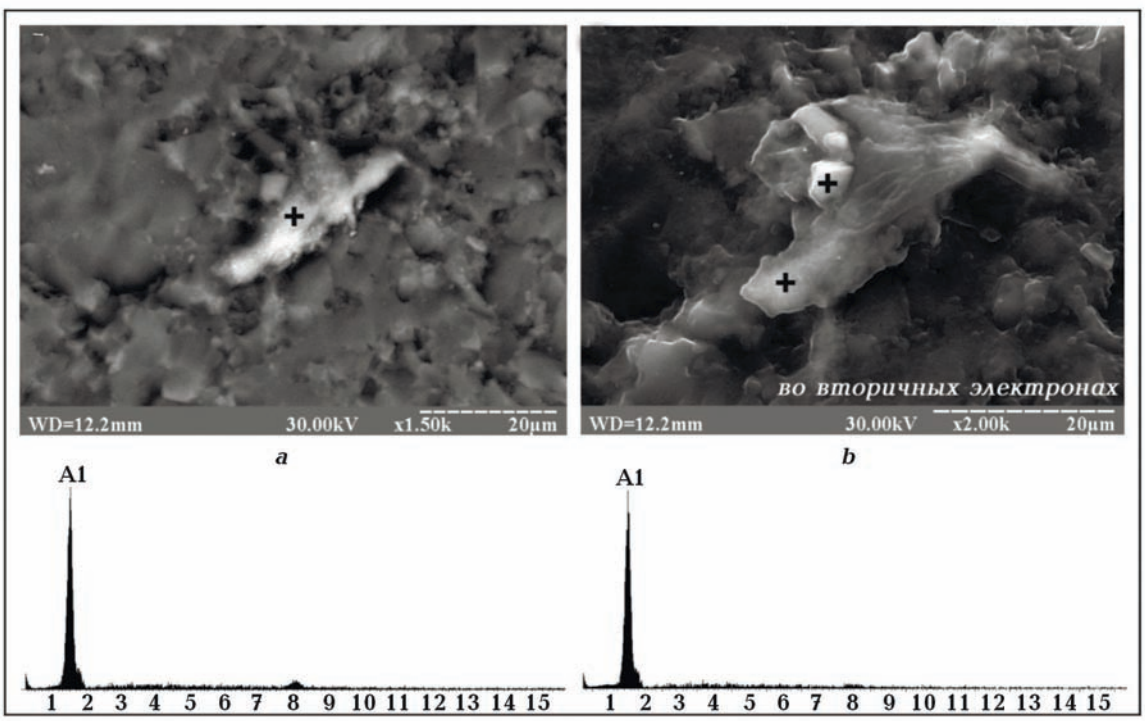

Fig. 3. Needle-lamellar aggregate (*a*) and film (*b*) of native Al in the oil-bearing dolomite of the Kuyumbinske field (East Siberia) (Borehole K-220, depth 2527.2—2533.3 m).

especially pronounced in this case (explosive factors of granite massif decompaction). All together, this reflects the unevenness of its distribution in the oil-and-gas-bearing reservoirs.

Reasonable grounds exist to believe that during the interaction of superdeep high-enthalpy dry hydrogen-hydrocarbon fluids with lithosphere rocks, a much broader range of elements, including silicon, the alkaline earth and the alkali metals, may appear in the native state. Despite their ephemeral existence, they can play an important catalytic role in the processes of endogenous mineral formation and organic synthesis. Apparently, the real extent of formation of native metals associated with trans-magmatic (and trans-hydrothermal) fluid flows was much greater, whereas in studying rocks and other mineral aggregates of the Earth's crust we only deal with their relics preserved due to the oxide passivating film and (poly)mineral isolating cover. It is fully applicable to aluminium. The extent of Al^0 formation during this interaction seems to be extremely large, as evidenced by the morphological diversity of its relic inclusions.

Assessment of possible pathways of native aluminum formation in the geological conditions of the Dnipro-Donetsk Basin by thermodynamic modeling. Thermodynamic modeling is widely used to study the processes of serpentinization of rocks with formation of hydrogen in a wide range of pH and *TP*-conditions [Olsen, 1963; Wetzel, Shock, 2000; Evans, 2004; Palandri, Reed, 2004; Sleep et al., 2004; McCollom, Bach, 2009; Leong et al., 2018, 2021a,b; Leong, Shock, 2020]. In this work, this method was used to estimate the possible ways of native aluminum formation as a result of interaction of hydrogen-bearing hot fluid with rocks in the conditions of the Dnipro-Donetsk Basin.

Modeling was carried out for different types of rocks: sedimentary rocks, weathering crust rocks, acid, intermediate, basic, and ultrabasic rocks. Table 1 presents the list of the rocks considered. Expected temperatures are estimated based on the assumption that the temperature increases by 3 degrees for every 100 m. Expected pressures are estimated based on the data presented in [Chirvinskiy, Cherkas, 1934].

The geological cross section for modeling was compiled from the Lelyakivske field data (upper part) and from the geophysical data (lower part). This approach is quite acceptable for obtaining a conceptual assessment of the possibility of NA formation in these rocks.

The depth of sedimentary and weathering crust rocks in the Dnipro-Donetsk Basin can reach 10 km. The rocks temperature exceeds the temperature of the water critical point (647.3 K) at depths below 10.8 km. The

Table 1. List of rocks considered, expected depths of occurrence, and *TP*-conditions

Type of rock	Rocks	Expected depth of occurrence, km	*T*, K	*P*, Pa
Sedimentary rocks	Arkose sandstones	0.5	313.15	8.53E+05
	Argillites	1	328.15	9.30E+05
	Dolomites	1.8	352.15	1.05E+06
	Quartz sandstones	4	418.15	1.39E+06
	Limestones	6	478.15	1.70E+06
	Domanikoids	8	538.15	2.01E+06
Weathering crust rocks	Kaolins	10	598.18	2.32E+06
Acidrocks	Granites, gneisses	10.5	647.15	2.57E+06
Intermediaterocks	Diorites	10.5	647.15	2.57E+06
Basicrocks	Gabbro	10.5	647.15	2.57E+06
	Basalts	10.5	647.15	2.57E+06
	Dolerites	10.5	647.15	2.57E+06
Ultrabasicrocks	Dunites	10.5	647.15	2.57E+06

modeling tool does not allow calculations under such conditions. Therefore, to assess the possibility of native Al formation in acid, intermediate, basic and ultrabasic rocks the calculations were performed at a temperature of 647.15 K and a pressure of 2.57E+06 Pa, which corresponds to a depth of 10.5 km. Under these conditions, water is in a vaporous state, and the *TP*-conditions do not exceed the technical capabilities of the modeling tool. Of course, this approach does not allow us to obtain reliable numerical values of the system parameters at which the native aluminium formation can occur. However, preliminary calculations have shown that there is no significant temperature and pressure influence on the interaction of the gas fluid with the rocks. This allows usto estimate the potential possibility of Al^0 formation in these rocks and assess the direction of system composition changing with changes in such parameters as the gas phase composition. Modeling was performed using the GEMS software package (http://gems.web.psi.ch/).

Input data. To perform the simulation using the GEMS software package, you need to set the following input data: a list of chemical elements that describe the model system; a list of phases that are present or can potentially form in the system; bulk chemical composition of system (total amount of chemical elements in the system that is specified either by the chemical composition of rocks, aqueous solution, and gas phase, or by the amount of chemical elements in the system); simulation temperature and pressure; thermodynamic data of the components of the model system phases.

According to Table 2 and Table 3, the model system is fully described by the set of elements Al, Si, Ca, Mg, Na, K, Fe, S, C, O, H, Cl. Chlorine is included in the model system for the series 4 calculations.

The bulk composition of the system was set by the chemical composition of rocks and gas fluids from Table 2 and Table 3.

The chemical composition of the gas fluid (see Table 3) was selected as close as possible

Table 2. Chemical and mineral composition of rocks

Rock	Chemical composition			Mineral composition	
	Component	Content, %		Mineral	Content, %
		Typical	Used for modeling		
Sedimentary rocks					
Arkose sandstones	SiO_2	70	70	Feldspars	60
	Al_2O_3	12	12	Quartz	30
	CaO	2	2	Micas	10
	Na_2O	3	3	—	—
	K_2O	8	8	—	—
Argillites	SiO_2	76.14	76.14	Hydromicas	60
	TiO_2	0.35	0.35	Chlorite	10
	Al_2O_3	7.44	7.44	Kaolinite	10
	Fe_2O_3	0.69	0.69	Siderite	10
	FeO	2.46	2.46	Calcite	5
	MnO	0.02	0.02	Pyrite	5
	MgO	1.58	1.58	—	—
	CaO	2.41	2.41	—	—
	Na_2O	0.52	0.52	—	—
	K_2O	2.20	2.20	—	—
	H_2O^+	2.33	2.33	—	—
	H_2O^-	0.38	0.38	—	—
	LOI	6.40	6.40	—	—
	CO_2	1.55	1.55	—	—
	P_2O_5	0.12	0.12	—	—
	S	0.32	0.32	—	—
	Corg	3.36	3.36	—	—

Rock	Chemical composition			Mineral composition	
	Component	Content, %		Mineral	Content, %
		Typical	Used for modeling		
Dolomite	CaO	30.4	30.4	Dolomite	100
	MgO	21.7	21.7	—	—
	CO_2	47.5	47.5	—	—
Quartz sandstones	SiO_2	72.31	72.31	Quartz	80
	TiO_2	0.49	0.49	Kaolinite	15
	Al_2O_3	16.03	16.03	(Admixtures: calcite, ankerite, ilmenite, pyrite)	<5
	Fe_2O_3	2.12	2.12		
	MgO	0.83	0.83		
	CaO	0.43	0.43		
	Na_2O	0.33	0.33	—	—
	K_2O	2.82	2.82	—	—
	P_2O_5	0.06	0.06	—	—
	SO_3	0.44	0.44	—	—
	LOI	4.39	4.39	—	—
Limestones	SiO_2	1.14	1.14	Calcite	85
	Al_2O_3	0.41	0.41	Dolomite	5
	MgO	0.26	0.26	Quartz	5
	CaO	54.84	54.84	Hydromicas	5
	CO_2	43.26	43.26	—	—
Domanikoids	SiO_2	45.51	45.51	Hydromicas	70
	TiO_2	0.57	0.57	Quartz	20
	Al_2O_3	12.10	12.10	Kerogen (Corg)*	~5
	Fe_2O_3	2.56	2.56	Siderite	<5
	MgO	0.51	0.51	—	—
	CaO	tr	0.05	—	—
	Na_2O	0.29	0.29	—	—
	K_2O	3.32	3.32	—	—
	H_2O	3.60	3.60	—	—
	P_2O_5	0.21	0.21	—	—
	S	0.40	0.40	—	—
	LOI	29.19	—	—	—
Weathering crust rocks					
Kaolins	SiO_2	60	60	Kaolinite	80
	Al_2O_3	19.75	19.75	Quartz	10
	Fe_2O_3	4.99	4.99	Hydromicas	5
	MgO	1.00	1.00	Siderite	5
	CaO	1.00	1.00	—	—
	Na_2O	0.10	0.10	—	—
	K_2O	1.20	1.20	—	—
	LOI	10	10	—	—
Acid rocks					
Granites, gneisses	SiO_2	68—73	70.5	Feldspars (acid plagioclase and K-feldspar)	60—65
	TiO_2	0.1—0.6	0.35		
	Al_2O_3	12.0—15.5	13.75		
	Fe_2O_3	0.5—2.5	1.5		
	FeO	0.5—3.0	1.75	Quartz	25—35
	MgO	0.1—1.5	0.8	Micas (biotite)	5—10
	CaO	1.5—4.0	2.75	—	—
	Na_2O	3.0—6.0	4.5	—	—
	K_2O	0.5—3.0	1.75	—	—
Intermediate rocks					
Diorites	SiO_2	53—58	55.5	Bright plagioclase	60—80
	TiO_2	0.3—1.5	0.9		
	Al_2O_3	14—20	17	Hornblende	5—40

Rock	Chemical composition			Mineral composition	
	Component	Content, %		Mineral	Content, %
		Typical	Used for modeling		
Diorites	Fe_2O_3	1.5—5	3.25	Pyroxene	5—20
	FeO	3—6	4.5	Biotite, quartz	up to 5
	MgO	0.8—6	3.4	—	—
	CaO	4—9	6.5	—	—
	Na_2O	2—6.5	4.25	—	—
	K_2O	0.3—2	1.15	—	—
Basic rocks					
Gabbro	SiO_2	43—52	47.5	Pyroxene	50
	TiO_2	0.1—4	2.05	Ca-plagioclase	50
	Al_2O_3	8—27	17.5	—	—
	Fe_2O_3	0.3—10	5.15	—	—
	FeO	1.5—15	8.25	—	—
	MgO	3—15	9	—	—
	CaO	8—18	13	—	—
	Na_2O	0.5—3.5	2	—	—
	K_2O	0.05—2	1.01	—	—
Basalts	SiO_2	47—52	49.5	Volcanic glass	50
	TiO_2	1—2.5	1.75		
	Al_2O_3	14—18	16	Basic	25
	Fe_2O_3	0.3—10	3.5	(Ca-plagioclase	
	FeO	6—10	8	Clinopyroxene	15
	MnO	0.1—0.2	—	Titanomagnetite	10
	MgO	5—7	6	—	—
	CaO	6—12	9	—	—
	Na_2O	1.5—3	2.25	—	—
	K_2O	0.1—1.5	0.3	—	—
	P_2O_5	0.2—0.5	—	—	—
Dolerites	SiO_2	46—49	47.5	Plagioclase	—
	TiO_2	1—2.5	1.75	Pyroxene	—
	Al_2O_3	12—17	14.5	Olivine	—
	Fe_2O_3	0.5—11	5.75	Quartz	—
	FeO	4—14	9	Magnetite	—
	MnO	0—0.3	—	Ilmenite	—
	MgO	7—15	11	Apatite	—
	CaO	6—13	9.5	—	—
	Na_2O	1.5—3.5	2.5	—	—
	K_2O	0.1—2	1.05	—	—
	P_2O_5	0—0.6	—	—	—
Ultrabasic rocks					
Dunites	SiO_2	35—40	37.5	Olivine	80
	TiO_2	up to 0.02	0.02	Chromite	15
	Al_2O_3	up to 2.5	2.5	Titanomagnetite	5
	Fe_2O_3	0.5—7	3.75	—	—
	FeO	3—6	4.5	—	—
	MgO	38—50	44	—	—
	CaO	up to 1.5	1.5	—	—
	Na_2O	up to 0.3	0.3	—	—
	K_2O	up to 0.25	0.25	—	—

*Not included in the model system

to the composition of natural gas [Bondarenko et al., 2005]. Depending on the tasks of the model calculation, its composition was changed by increasing the amount of hydrogen, methane, and adding aluminium.

The phase composition of the system is

Table 3. Chemical composition of gas fluid

Component	Content, %
CH_4	97.8
C_2H_6	0.5
C_3H_8	0.2
C_4H_{10}	0.1
H_2	0.7
H_2S	0.7

formed based on the data presented in Table 2 and based on the assumption that the system contains a solids and gas phases. Depending on the purpose of modeling, aqueous phase may be present.

The systems include: mineral phases (Table 4), described as simple minerals (minerals of constant composition) and solid solutions (minerals of variable composition); the gas phase described as a mixture of ideal gases;

Table 4. Mineral phases included for different types of rocks

Phase	Formula	System												
		ark	argl	dol	qss	ls	dom	kln	gr	dio	gb	bas	dole	dun
Simple minerals														
Aluminium	Al^0	+	+	+	+	+	+	+	+	+	+	+	+	+
Boehmite	AlOOH	+	+	+	+	+	+	+	+	+	+	+	+	+
Gibbsit	$Al(OH)_3$	+	+	+	+	+	+	+	+	+	+	+	+	+
Aragonite	$CaCO_3$	+	+	+	+	+	+	+	+	+	+	+	+	+
Calcite	$CaCO_3$	+	+	+	+	+	+	+	+	+	+	+	+	+
Dolomite	$CaMg(CO_3)_2$	+	+	+	+	+	+	+	+	+	+	+	+	+
Anhydrite	$CaSO_4$	+	+	+	+	+	+	+	+	+	+	+	+	+
Gypsum	$CaSO_4 \cdot 2H_2O$	+	+	+	+	+	+	+	+	+	+	+	+	+
Iron	Fe^0	+	+		+	+	+	+	+	+	+	+	+	+
Fe-carbonate	$FeCO_3$	+	+		+	+	+	+	+	+	+	+	+	+
Siderite	$FeCO_3$	+	+		+	+	+	+	+	+	+	+	+	+
Hematite	Fe_2O_3	+	+		+	+	+	+	+	+	+	+	+	+
Magnetite	Fe_3O_4	+	+		+	+	+	+	+	+	+	+	+	+
Goethite	FeOOH	+	+		+	+	+	+	+	+	+	+	+	+
Pyrite	FeS_2	+	+		+	+	+	+	+	+	+	+	+	+
Ilmenite	$FeTiO_3$	+	+		+	+	+	+	+	+	+	+	+	+
Kaolinite	$Al_2Si_2O_5(OH)_4$	+	+					+						
Microcline	$KAlSi_3O_8$	+							+	+	+	+		
Muscovite	$KAl_3Si_3O_{12}H_2$	+												
Magnesite	$MgCO_3$	+	+	+	+	+	+	+	+	+	+	+	+	+
Brucite	$Mg(OH)_2$	+	+	+	+	+	+	+	+	+	+	+	+	+
Mg-Silicide	Mg_2Si	+	+		+	+	+	+	+	+	+	+	+	+
Sulfur	S^0	+	+	+	+	+	+	+	+	+	+	+	+	+
Quartz	SiO_2	+	+		+	+	+	+	+	+	+	+	+	+
Silica	SiO_2am	+	+		+	+	+	+	+	+	+	+	+	+
Titanium	Ti^0	+	+		+	+	+	+	+	+	+	+	+	+
Solid solutions														
Plagioclase	Anorthite	+							+	+	+	+	+	
	Albite	+							+	+	+	+	+	
Ca-clinopyroxene	Ca-chermakite									+	+	+	+	
	Hedenbergite									+	+	+	+	
	Diopside									+	+	+	+	
	Jadeite									+	+	+	+	

Phase	Formula	System												
		ark	argl	dol	qss	ls	dom	kln	gr	dio	gb	bas	dole	dun
Na-clinopyroxene	Hedenbergite									+	+	+	+	
	Diopside									+	+	+	+	
	Jadeite									+	+	+	+	
	Acmite									+	+	+	+	
Ca-amphibole	Tremolite									+			+	
	Fe-actinolite									+			+	
	Chermakite									+			+	
	Pargasite									+			+	
	Glaucophane									+			+	
	K-pargasite									+			+	
	Fe-glaucophane									+			+	
Na-amphibole	Glaucophane									+			+	
	Fe-glaucophane									+			+	
	Riebeckite									+				
Titanomagnetite	Magnetite	+	+	+	+	+	+	+	+	+	+	+	+	+
	Ulvospinel	+	+	+	+	+	+	+	+	+	+	+	+	+
Olivine	Fayalite												+	+
	Forsterite												+	+
Chlorite	$Fe_{4.4}Al_{3.2}Si_{2.4}$		+						+					
	$Fe_{4.4}Fe_{1.6}Al_{1.6}$		+						+					
	$Mg_4Al_4Si_2$		+						+					
	$Mg_5Al_2Si_3$		+						+					
	$Mg_4Fe_2Al_2Si_2$		+						+					
	$Mg_5FeAlSi_3$		+						+					
Biotite	Annite								+	+				
	Phlogopite								+	+				
Illite	$Al_2Si_4O_{12}$		+			+	+	+						
	$Ca_{0.5}Al_3Si_3O_{12}H_2$		+			+	+	+						
	$KAl_3Si_3O_{12}H_2$		+			+	+	+						
	$KFe_3AlSi_4O_{12}H_2$		+			+	+	+						
	$KFeAlSi_4O_{12}H_2$		+			+	+	+						
	$KMg_3AlSi_4O_{12}H_2$		+			+	+	+						
	$NaAl_3Si_3O_{12}H_2$		+			+	+	+						
Serpentine	Greenalite								+				+	+
	Chrysotile								+				+	+
Smectite	$Al_2Si_4O_{12}$		+			+								
	$Ca_{0.5}Al_3Si_3O_{12}H_2$		+			+								
	$Fe_2Si_4O_{12}$		+			+								
	$Fe_3Si_4O_{12}$		+			+								
	$KAl_3Si_3O_{12}H_2$		+			+								
	$Mg_3Si_4O_{12}$		+			+								
	$NaAl_3Si_3O_{12}H_2$		+			+								

Note: ark — Arkose sandstones; argl — Argillites; dol — Dolomites; qss — Quartz sandstones; ls — Limestones; dom — Domanikoids; kln — Kaolins; gr — Granites, gneisses; dio — Diorites; gb — Gabbro; bas — Basalts; dole — Dolerites; dun — Dunites.

water solution phase (only included for some series of calculations).

The composition of the gas and aqueous (in case it is included in the model system according to the purposes of modeling) phases was the same for all rocks. The composition of the mineral phases was formed concretely for each type of rock based on their mineral composition (see Table 2). Also were included minerals that can potentially form in systems during rock interaction with gaseous and water fluids.

The models of solid solutions from [Avchenko et al., 2009] were used to describe Ca-clinopyroxene, Na-amphibole, Ca-amphibole, and titanomagnetite. Olivine and serpentine were also described by solid solutions models [Shestopalov et al., 2022] as well as illite and smectite [Koliabina et al., 2009]. Other solid solutions models were already included in the GEMS database.

The gas phase includes CO_2, CH_4, H_2, O_2, H_2S, SiH_4, H_2O. The aqueous phase includes: water, hydrogen and hydroxide ion; simple ions (Me^{z+}, HS^-, S^{2-}, HSO_4^-, SO_4^{2-}, HCO_3^-, CO_3^{2-}, ClO_4, Cl^-) and undissociated acids (H_2S^0, $H_2SO_4^0$, CO_2^0); hydroxide, sulfate, sulfide, carbonate, hydrocarbonate complexes of Al, Si, Ca, Mg, Na, K, Fe; gases dissolved in water (H_2, CH_4, O_2).

The thermodynamic data for all components of the aqueous, gas, and most mineral phases were already included in the GEMS database. Thermodynamic data from [Naumov et al., 1971] were used for end members of solid solution models of pyroxenes (hedenbergite, jadeite, acmite), and amphiboles (chermakite, pargasite, glaucophane, K-pargasite, Fe-glaucophane, riebeckite).

GEMS uses the HKF equation [Shock, Helgeson, 1988; Shock et al., 1997] and the isocoulombic reaction method [Gu et al., 1995] for extrapolating the thermodynamic properties of aqueous phase components to temperatures and pressures other than standard. The dependence $C_p=f(T)$ for the components of the gas phase and most minerals is described by a 12-term isobaric heat capacity equation (http://gems.web.psi.ch/). GEMS automatically recalculates thermodynamic parameters for the required *TP*-conditions.

The input data for each task are considered in more detail in the relevant sections below.

Simulation scenarios. Preliminary calculations have shown that under estimated *TP*-conditions (see Table 1) the native aluminium-does not form without addition of Al during certain rocks (arkose sandstones, argillites, dolomite, quartz sandstones, and limestone) interaction with a fluid. Under typical *TP*-conditions for these rocks (Fig. 4, orange dots), the water is in a liquid state, which causes the formation of boehmite.

Native aluminium forms in a wide range of gas fluid compositions in acidic, intermediate, basic, and ultrabasic rocks. In the *TP*-conditions specific for these rocks (Fig. 4, green dots), water is in a vaporous state, which, apparently, partially prevents the boehmite formation.

Preliminary calculations also showed that the main factor affecting the native aluminium formation is the aluminium and hydrogen concentration in the fluid. The temperature and pressure influence was negligible. Pressure and temperature only affected the rock minerals ratio and the hydrocarbons ratio. Temperature also influenced the phase state of water. The methane concentration in a fluid also had a negligible effect. With this in mind, several series of calculations were performed:

Series 1. Calculation of the mineral composition of systems under the expected rock *TP*-conditions and at elevated temperatures.

Series 2. Estimation of the aluminium concentration in the gas fluid necessary for native aluminium formation in rocks.

Series 3. Evaluation of the effect of gas fluid composition and temperature on the native aluminiumformation.

Series 4. Assessment of the impact of the return of natural conditions to the initial state after the passage of the gas fluid through the rocks on the formed native aluminiumand boehmite.

Results. ***Series 1. Calculation of the mineral composition of systems under the expected T-P conditions of rocks and at elevated temperatures.*** As noted above, the native aluminium does not form in arkose sandstones,

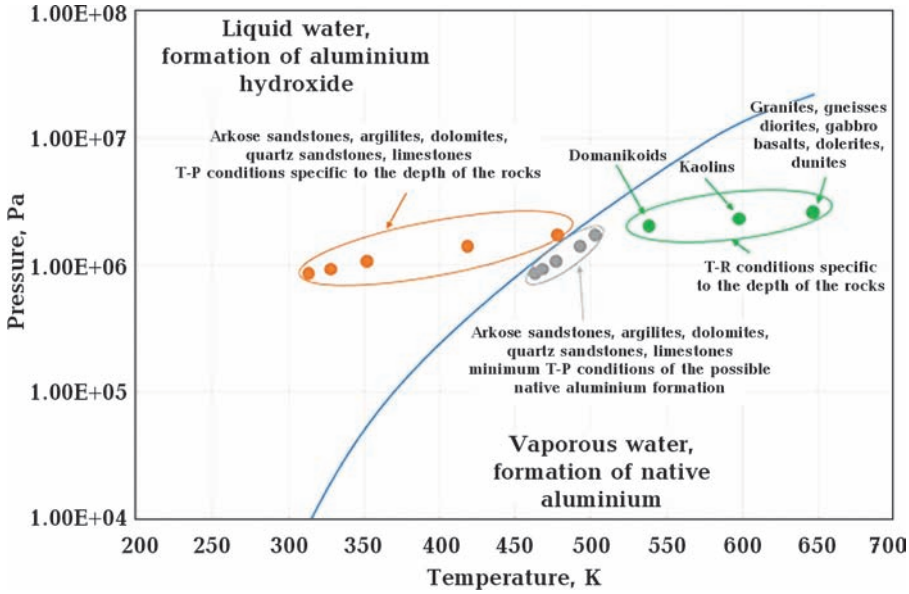

Fig. 4. Scheme of the *TP*-coordinates of the simulation points.

argillites, dolomite, quartz sandstones, and limestone (Fig. 4, orange dots) because of the liquid state of water under the expected *TP*-conditions of rocks. Therefore, the modeling of the mineral composition of these rocks was performed for two temperatures — the expected *T* (water is in a liquid state), and the elevated *T*, when water is in a vapor state at this pressure (gray dots in Fig. 4, Table 5).

In all calculations, the chemical composition of the system was set by the chemical composition of 1 kg of rock (see Table 2). A gas phase without Al (see Table 3) was added to the system in calculations at elevated temperatures. The calculations were carried out at the same temperature without and with addition of the Al-free gas fluid for domanikoids, kaolins, acid, intermediate, basic, and ultrabasic rocks. It was assumed that the liquid water evaporates during the interaction of rocks with gas fluid under *TP*-conditions of vapor water.

The simulation results showed (Fig. 5) that the mineral composition calculated for the expected *TP*-conditions is in good agreement with the measured values. Insignificant dif-

Table 5. *TP*-conditions for calculations of series 1

Rock type	Rocks	*P*, Pa	Expected *T*, K	Increased *T*, K
Sedimentary rocks	Arkose sandstones	8.53E+05	313.15	463.15
	Argillites	9.30E+05	328.15	468.15
	Dolomite	1.05E+06	352.15	477.15
	Quartz sandstones	1.39E+06	418.15	488.15
	Limestones	1.70E+06	478.15	493.15
	Domanikoids	2.01E+06	538.15	503.15
Weathering crust rocks	Kaolins	2.32E+06	598.18	—
Acidrocks	Granites, gneisses	2.57E+06	647.15	—
Intermediaterocks	Diorites	2.57E+06	647.15	—
Basicrocks	Gabbro	2.57E+06	647.15	—
	Basalts	2.57E+06	647.15	—
	Dolerites	2.57E+06	647.15	—
Ultrabasicrocks	Dunites	2.57E+06	647.15	—

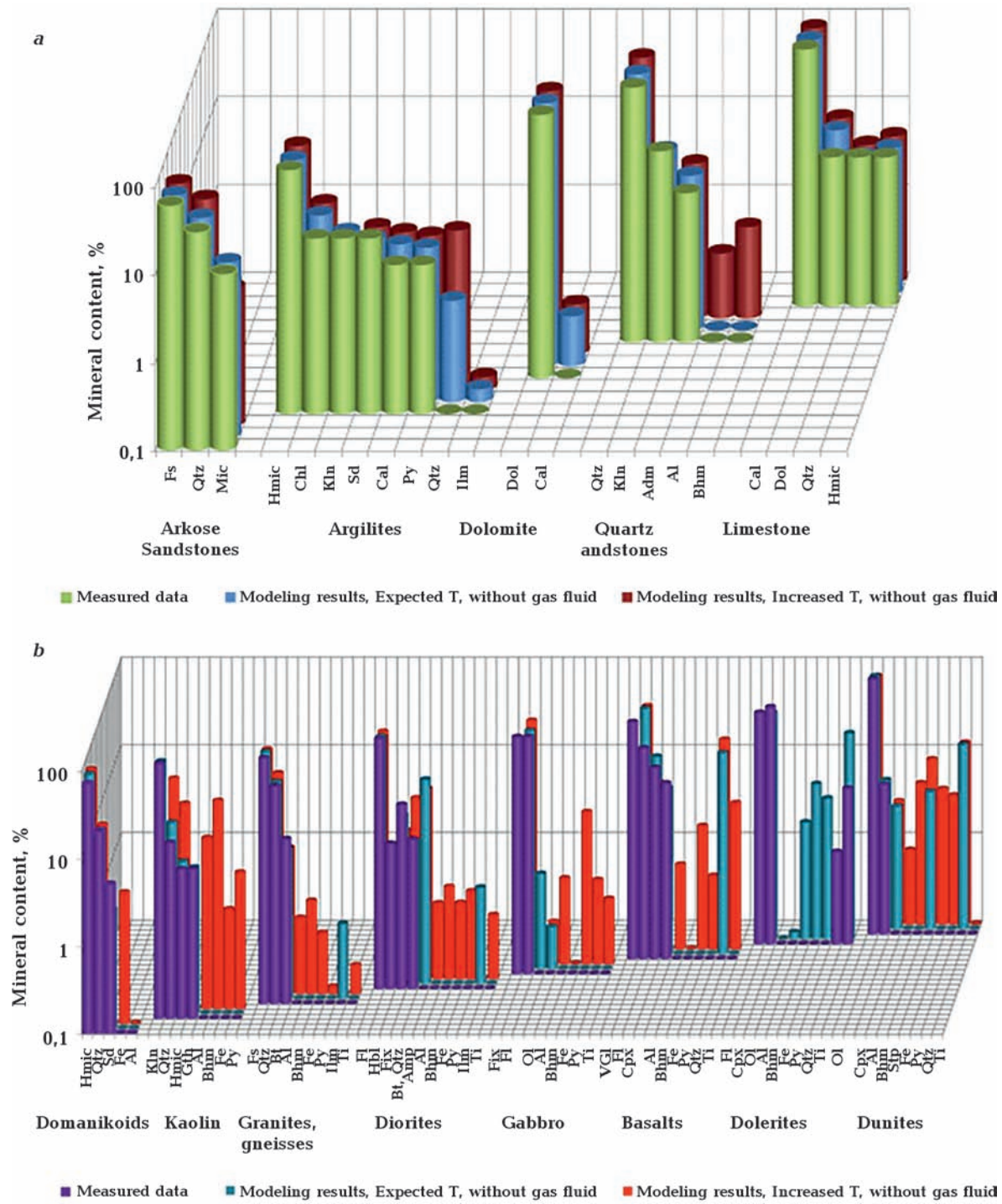

Fig. 5. Mineral composition — comparison of modeling results and measured data: *a* — sedimentary rocks; *b* — domanicoids, weathering crust rocks, acid, intermediate, basic and ultrabasic rocks (Fs — Feldspar, Qtz — Quartz, Mic — Micas, Hmic — Hydromica, Chl — Chlorite, Kln — Kaolinite, Sd — Siderite,Cal — Calcite, Py — Pyrite, Ilm — Ilmenite, Dol — Dolomite, Adm — Admixtures (calcite, ankerite, ilmenite, pyrite), Bhm — boehmite).

ferences between the simulation results and measured data may arise due to inaccuracies in the extrapolation of thermodynamic values to high temperatures and pressures, and also as a consequence of using ideal solid solutions models for minerals of variable composition. We should note that the use of ideal solid solutions models is more accurate than their

replacement by simple minerals. Good agreement between the simulation and measured data confirms this as well.

Significant differences exist in the mineral composition of rocks under *TP*-conditions of vapor water (Fig. 5, *a*). Temperature rising to *TP*-conditions of vapor water,as well as the addition of gas fluid has little effect on the mineral composition of arkose sandstones, dolomites and limestones. Kaolinite decomposes in kaolinite-bearing rocks (argillites, quartz sandstones) in the presence of gas fluid under *TP*-conditions of vapor water. Additional quartz, native aluminium and boehmite are formed in quartz sandstones, while illite is formed in argillites. Illite is not formed in quartz sandstones due to the lack of sufficient K, Na, Ca and Mg in their chemical composition. Additional illite, native Al and boehmite are formed in kaolins in the presence of gas fluid (Fig. 5, *b*).

It should be noted that native Al formation in large quantities due to the rocks-gas fluid interaction in kaolins and quartz sandstones is doubtful under the *TP*-conditions of vapor water. Some phases (minerals), which can influence the amount of aluminiumformed, are probably not included in the system. At the current stage of research, no information is available to include additional mineral phases, so we cannot draw a correct conclusion about the possibility of native Al formation in these rocks.

In addition, small quantities of native Al form in domanikoids as a result of the rock-gas fluid interaction under *TP*-conditions of vaporous water. However, the model system did not include a kerogen. This pruning may affect the native Al formation. So, we cannot estimate clearly the possibility of Al generation in these rocks.

Native aluminiumdoes not form in other sedimentary rocks due to rock-gas fluid interaction under *TP*-conditions of vaporous water. The estimation of additional Al concentration in gas fluid required fornative aluminium generation is given below. Small amount of native aluminium forms without adding Al in all acidic, intermediate, basic, and ultrabasic rocks as a result of rock-gas fluid interaction.

It should be noted that iron and titanium minerals decompose as a result of rock-gas fluid interaction under *TP*-conditions of vapor water in all rocks. In this process, metallic Fe, Ti, pyrite are formed.

Series 2. Estimation of the aluminium concentration in the gas fluid required for Al^0 formation in rocks. The results presented above showed that native aluminium did not form under *TP*-conditions of vapor water in four types of sedimentary rocks (arkose sandstones, argillites, dolomites, and limestones). We suppose the possibility of native Al formation in the presence of additional aluminium in gas fluid. We estimated the required aluminium quantity by simulation of the influence of Al concentration in the gas fluid on the native aluminium formation.

Simulations were performed for *TP*-conditions of vapor water using the model systems described above. It was assumed that all the water passes into a vapor state.

The results showed that when additional Al arrives with gas fluid, the native aluminium forms in all sedimentary rocks. As noted above, native aluminium is produced without additional Al in quartz sandstones, domanikoids, kaolins, as well as in acidic, intermediate, basic, and ultrabasic rocks.

At the same time, boehmite forms along with native aluminium in most rocks. Boehmite can create a protective oxide film around aluminium and prevent it from further oxidation. The exceptions are domanikoids, gabbro, and basalts, in which boehmite does not form.

The modeling results show that required Al content in gas fluid exceeds 1 % in arkose sandstones (1.8 %), argillites (5.17 %), and limestones (1.8 %), which does not seem realistic. So, the most probable is deposition of native aluminium in dolomitesin which the required Al content in gas fluid is 0.08 %. Therefore, dolomites were considered only in subsequent assessments. In addition, since geologic evidence of metallic aluminium is only available for basalts, further modelingwasperformedexclusively for these rocks.

The question arises as to the possible nature of the Al in the gas fluid. Underlying

rocks are unlikely to be a source of aluminium for the gas fluid because the native aluminium is deposited as a result of rock-fluid interaction and the fluid is depleted rather than enriched in aluminium. Even if we assume that the interaction process ended in a given volume and does not develop radially away from the interaction zone, these rocks can hardly be a source of aluminium for the gas fluid. There are a number of reasons for this. Firstly, none of the rocks produces enough aluminium to pass into the gas fluid in the amount necessary to form aluminium in limestones, argillites, and sandstones. Secondly, the modeling results showed that the native aluminium formation increases with increasing Al concentration in the fluid in all rocks, including those in which native aluminium is generated even in its complete absence in the fluid. Hence, even if metallic aluminium formed in the underlying rocks passes into the gas fluid, it can be deposited in the overlying rocks and not reach the sedimentary rocks. Thus, the most probable aluminium source in the gas fluid is the mantle.

Series 3. Evaluation of the effect of gas fluid composition and temperature on the native aluminium formation. For the reasons stated in the previous paragraphs, this calculation series was carried out only for dolomites and basalts. The simulations were performed using the model systems described above.

Comparison of the formation of native aluminium during rock interaction with a hydrocarbon-containing fluid and with a pure hydrogen fluid.

The modeling results showed that both in basalts (native aluminium forms in no presence of Al in gas fluid) and in dolomites (native aluminium forms only in the presence of Al in gas fluid), the hydrocarbons concentration in the fluid does not affect the native aluminium formation (the modeling results differ in the eighth decimal point).

This indicates that methane, the main component of natural gas, is not involved in the formation of native Al under the considered *TP*-conditions, which is consistent with published data from other researchers in the development of aluminium production technologies [e.g., Rains, Kadlec, 1970; Petrasch, 2002; Halmann et al., 2012; Kulongoski et al., 2018, etc.]. In further calculations, the composition of gas fluid from Table 3 was used. Additional hydrogen or aluminium was added depending on the calculation purpose.

Effect of hydrogen concentration in gas fluid on the native aluminium formation, the ratio of hydrocarbons, and mineral composition of rocks.

In dolomites, in which native aluminium can only be formed through Al ingress with gas fluid, a required aluminium concentration in gas fluid decreases from 0.08 % at H_2=0.7 to 0.01 % at H_2=100 % as the hydrogen concentration in the fluid increases above 5 % (Fig. 6).

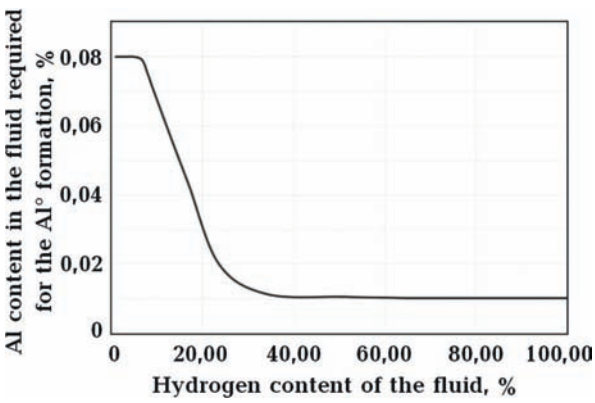

Fig. 6. Relationship between required Al concentration and hydrogen concentration in the fluid.

The hydrogen concentration in the fluid has only a minor effect on the native Al formation in basalt, where it can form without adding Al in the gas fluid. Nevertheless, the native aluminiumformation increases weakly with increasing Al concentration in the fluid. The concentration of the concurrently formed boehmite varies even less. Also, an increase in the amount of hydrogen affects the ratio of iron minerals (Fig. 7). The Fe-minerals ratio does not change up to the hydrogen concentration in the fluid of 5 mol. As H_2 concentration continues to rise, the quantity of Al^0 increases and that of boehmite decreases. The boehmite concentration practically drops to zero at a hydrogen concentration of 322 mol.

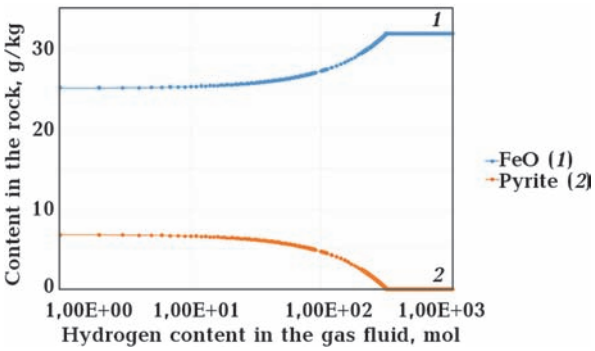

Fig. 7. Dependence of the iron minerals ratio in basalt on the hydrogen concentration in the fluid.

The hydrocarbons ratio in the fluid influences insignificantly the formation of Al^0 in both basalt and dolomite.

The hydrogen concentration affects considerably the ratio of natural gas components in the fluid, and this effect is different for dolomites and basalts. In dolomites, the C_3H_8, C_2H_6, and C_4H_{10} concentration increases, while the CH_4 concentration decreases with an increase in hydrogen concentration. In basalts, on the contrary, the C_3H_8, C_2H_6, and C_4H_{10} concentration decreases, and CH_4 concentration increases with an increase in hydrogen concentration. It should be noted that at the specific hydrogen concentration in the fluid, the C_3H_8 and C_4H_{10} concentration in basalts decreases below $1{\cdot}10^{-9}$, which is on the verge of calculations reliability and usability of the method of thermodynamic modeling. So, we can assume that the C_3H_8 and C_4H_{10} concentration becomes equal to 0. Thus, in basalts, C_4H_{10} occurs only at the hydrogen concentrations in the gas fluid less than 4 moles, and C_3H_8 — only at the hydrogen concentrations less than 80 moles.

Such contradiction between dolomites and basalts can be determined primarily by different chemical composition of the rocks (see Table 2).The CO_2 content in dolomites is 47.5 %, while no CO_2 is found in basalts. So, dolomites have an additional source of carbon, providing an increase in the concentration of hydrocarbons with longer carbon chains in the gas phase. In contrast, no additional source of carbon exists in the basalts, which leads to an increase in the methane concentration with a minimum degree of carbon oxidation.

Increasing the temperature above the necessary value to keep water in the vapor state has practically no effect on the formation of Al^0. A slight trend is observed towards an increase in the amount of Al^0 formed as the temperature rises, but the quantitative changes do not exceed 10^{-6} %.

Series 4. Assessment of the impact of the natural conditions returning to the initial state after the passage of gas fluid through the rocks on the formed native aluminium and boehmite. The above calculations showed that Al^0 forms along with boehmite in dolomite and basalts. However, the modeling method used gives quantitative estimates of the phases and does not allow taking into account in what form the minerals coexist in real conditions. It is well known that hydroxide (oxide) films form on the aluminium surface under favorable conditions. These films protect Al^0 from further oxidation [e.g., Smith, 1972; Lukin et al., 2007; Wang et al., 2009; Porciúncula et al., 2012, etc.]. It would be logical to assume the formation of boehmite protective film on the native aluminium surface, which will protect it from further oxidation.

Therefore, to assess the boehmite protective potential, simulation of its dissolution was performed in the conditions of the rocks returning to the natural state and their gradual saturation with water. The assessment was performed only for dolomite for expected *TP*-conditions given in Table 1 (indicated by orange dots in Fig. 4). Calculations were carried out for 100, 200, 300, and 400 g of liquid water in the system.

The simulations showed (Table 6) that the boehmite content in the rocks does not change virtually for all considered water amounts. This result suggests that even during multiple films interaction with water at a given *T* and *P*, boehmite will remain practically unchanged, which can provide long-term protection of Al^0 from oxidation. The low aluminiumconcentration in the equilibrium solution ($<2{\cdot}10^{-5}$ g/l) may confirm this.

Discussion. The above results allow us to make the following considerations. The na-

Table 6. Influence of the amount of water in the dolomite on the boehmite content

Boehmite content, g				
Vapor water *TP*, no liquid water	Liquid water *TP*			
	100 g H_2O	200 g H_2O	300 g H_2O	400 g H_2O
47.40	47.40	47.40	47.40	47.40

tive aluminium formation through the interaction of sedimentary rocks with gas fluid requires the *TP*-conditions of vapor water. This is quite possible in natural conditions, because the temperature of gas fluid coming from great depths is much higher than that of the sedimentary rocks. Although the calculations were performed under temperatures not exceeding 647.3 K (374.15 K), the absence of significant temperature dependence of native aluminium formation allows us to consider the obtained results as indicative for higher temperatures as well.

Formation of Al^0 in acid, intermediate, basic and ultrabasic rocks, as well as in some sedimentary rocks (quartz sandstones, domanicoids) and weathering crust rocks (kaolins) can occur through the interaction with the gas fluid under *TP*-conditions of water vapor. In this case, no additional aluminium input with the fluid is required.

The native aluminium formation in most sedimentary rocks (arkose sandstones, argillites, dolomites, and limestones) requires an additional aluminium input with the gas fluid. It is unlikely that the source of additional aluminum will be crustal rocks below, because native aluminum is deposited du to the rock-fluid interaction, and the fluid is depleted rather than enriched in aluminum. At the same time, the aluminum-containing fluid with excess pressure continues radially penetrating into the rock along the deconsolidation zones, losing aluminum. Even assuming that the interaction process is completed in a given volume and does not radially develop from the interaction zone, it is unlikely that these rocks can be a source of aluminum for the gas fluid. On the one hand, the amount of aluminium they produce is insufficient for the formation of Al^0 in the overlying sedimentary rocks. On the other hand, even if Al^0 formed in the dunite is then transferred to the gas fluid, it will be deposited in dolerites, granites and other rocks above. Thus, the most probable source of additional aluminium in the gas fluid is the mantle. Additional evidence for transition of reducing hot gas fluid through rocks may be the decomposition of iron and titanium minerals under *TP*-conditions of vapor water to form metallic Fe and Ti, as well as pyrite in some rocks.

Formation of boehmite in sedimentary rocks in parallel with Al^0 suggests that native aluminium may be covered with passivating films to protect it from further oxidation during the restoration of natural conditions when, after the hot gas fluid has passed through, the rock gradually cools down and the water returns to the liquid state.

In general terms, the formation of native aluminium in rocks can be described as follows.

As hot fluid from the mantle passes through, the rocks are heated. In sedimentary rocks, the *TP*-conditions, which originally corresponded to water in a liquid state, gradually turn to those with water in a vapor state, and strongly reducing conditions are formed due to hydrogen. Accordingly, water evaporates and the interaction of rocks with the ascending aluminium-bearing fluid results in the formation of Al^0, which is covered by a stable protective film of boehmite. Gradually, as rocks cool down after the hot fluid flows through them, the rocks return to *TP*-liquid water conditions and become saturated with water. However, presence of a protective film prevents oxidation of the formed native aluminium for a long time. Apparently, during periods of activation of tectonic stresses and violation of the protective film continuity a part of the NA was oxidized.

Additional evidence of the reducing hot fluid flow through the rocks may be the presence of native iron, titanium and other metals

and their melts, which are not addressed in this paper, but have been discussed previously in a number of works by different authors [e.g. Moody, 1976; Zucchetti et al., 1988; Peretti et al., 1992; González-Jiménez et al., 2021].

The results of an additional series of calculations, not included in this paper, showed that in the presence of CO_2 native aluminium is formed in the gas fluid at significantly higher concentrations of it, which are quite unlikely in natural conditions. This is because CO_2 is reduced to CH_4. In the presence of H_2O no Al^0 is formed in the gas fluid — only boehmiteis formed. These results are fully consistent with the conclusions reported in [Oleynikov et al., 1978; Novgorodova, 1979, 1983] and many others.

Methane, the main component of natural gas, is not involved in the native aluminium formation under the *TP*-conditions discussed. This indicates that Al^0 found in hydrocarbon fields is formed not from the dominant reduced gaseous compounds of carbon, but exclusively through the direct interaction between hydrogen coming with the hot gas fluid and rocks.

The paper [Dekov et al., 2009] presents data on the Al^0 flake protruding from the phlogopite matrix of a rock sample taken from a desilicized pegmatite vein intruded between a small serpentinized ultrabasic body and biotite gneiss. The authors suggest that two processes may have played a key role in the formation of Al^0: (1) desilication of the pegmatite resulting in Al enrichment; and (2) serpentinization of the ultrabasic body that created a strongly reduced front towards the serpentinite/pegmatite contact. These processes presumably led to the Al reduction to Al^0 in some parts of the alumina-rich minerals. Under extremely reducing conditions, the serpentinization process by the Fischer-Tropsch type reaction [Berndt et al., 1996; Sleep et al., 2004] produces H_2 and CH_4. These reduced gases, while migrating from the serpentinized ultrabasic body through the desiliconized pegmatite, reduced aluminium to Al^0 atcertainpoints, where Al-rich minerals occurred and the oxide cover on the Al^0 surface protected it from subsequent changes. The authors' key positions are the presence of liquid fluid (water) and serpentinization of mafic/ultramafic rocks according to the generally accepted scheme with formation of serpentine, Fe-brusite ($Fe_xMg_{(1-x)}(OH)_2$) and obligatory release of hydrogen [e.g., Janecky, Seyfried, 1986; Frost, Beard, 2007; McCollom, Bach, 2009; Klein et al., 2009; McCollom et al., 2016, 2020]. However, these processes are of relatively slow diffuse nature. We studied another case, in which hydrogen is not a product of rock-water interaction, but serves as an initiator of the rock modification process under the action of the ascending gas fluid with its high concentration [Shestopalov et al., 2022].

Formation of gaseous compounds of aluminium with chlorine, such as AlCl subchloride, is broadly discussed in current scientific literature as an obligatory intermediate stage of aluminium transport in the gas phase and deposition of native aluminium in various geological conditions [e.g., Iyer et al., 2007; Chen et al., 2011; Silaev at al., 2017; Paar et al., 2019, etc.]. The patent of Othmer D. F. [Othmer, 1974], which was mentioned in [Paar et al., 2019], deals with formation of AlCl from the interaction of Al_2O_3 with gaseous chlorine in the presence of C, its stability at temperatures of 1000—1200 °C and disproportionation into metallic aluminium and gaseous $AlCl_3$ at temperatures below 700 °C. Under the conditions, we considered (including natural gas composition) gaseous chlorine is not found. Its occurrence in natural water does not suggest the formation of AlCl even at appropriate temperature conditions, since according to [Othmer, 1974] water in the system combines with the existing chlorine to form hydrogen chloride, which can no longer serve as a reducing agent for Al_2O_3.

According to the modeling results, CH_4 is not involved in the aluminium reduction process, which is primarily explained by the energy stability of methane molecules [e.g., Hasnan et al., 2020; Bajec et al., 2020, etc.]. In addition, calculations [Halmann et al., 2012] showed that the formation of Al (g) from Al_2O_3 as a result of interaction with methane

is only possible at very high temperatures (>2000 °C). In the process, CH_4 is completely decomposed, which is inconsistent with the actual detection of native aluminum in the natural gas fields, being discussed in this paper.

Calculations demonstrated that the hydroxide films formed during recovery of the water content of rocks provide long-term protection for the aluminium formed. Aluminium and its alloys are known to be corroded by water containing aggressive anions, especially chloride solutions, even at low temperatures [e.g., Vijh, 1988; McCafferty, 2003; Naeini at al., 2011; Febrianto et al., 2019; Peng et al., 2022, etc.]. Moreover, it was reported that films formed on the surface of aluminium and its alloys also undergo point corrosion (pitting) by chloride solutions [e.g., Foroulis et al., 1975; Yu et al., 2000; Kolics et al., 2001; Li et al., 2013, 2017, etc.]. Temperature, pH, chlorine concentration and film thickness are the key factors which determine the rate, magnitude and depth of film corrosion. The diffusion of chlorine ions through the protective film is often considered to be the key determining process for the corrosion rate [e.g., Li et al., 2017, etc.]. The modeling software we used does not allow us to consider the kinetic features of the processes. We can therefore assume that the initial amount of metallic aluminium formed was actually higher, but due to corrosion the aluminium changed to other mineral forms and possibly was transported out of the system with the groundwater flow. The native aluminium particles we recorded were probably preserved due to their embedding in the rock structure in places poorly accessible to chloride natural water, where the corrosion of particles (or films on their surface) is limited not by the diffusion rate of chloride ions but by the rate of water inflow to the particle. In addition, the geological history of the study area is likely to alternate between periods of rock saturation with water and periods of rock drainage, thus disrupting diffusion processes.

It should be noted that in the axial part of the Dnipro-Donetsk Basin a rift of mantle origin is located (Fig. 8). More than 220 hydrocarbon fields are associated with its mantle faults and adjacent deformations, as well as with explosion ring structures within the rift. This constitutes only one fifth of the hydrocarbon potential of the basin [Lukin et al., 2020]. This potential was formed in the relatively recent geological history due to a giant hydrogen blowing of carbon-containing mantle rocks [Shestopalov et al., 2018, 2022]. Apparently, such blowing occurred repeatedly during the rift history and was of a periodic, pulsating nature. Well sampling shows that these deposits contain admixtures of unspent hydrogen. Besides, the hydrogen also forms independent seeps to a shallow depth [Lukin, Shestopalov, 2021; Shestopalov et al., 2022].

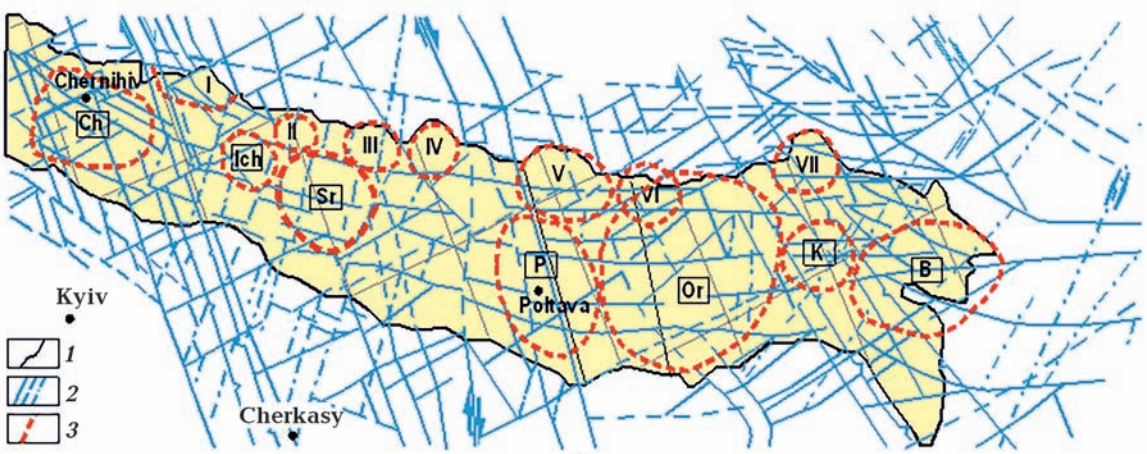

Fig. 8. Dnipro-Donetsk Rift (shaded yellow) (*1*) and deep faults from geophysical data (*2*), explosion ring structures within the rift boundaries (*3*).

The data available [Lepigov et al., 2011] indicate that degassing and fluid recharge pulses have occurred many times and are still occurring.

To summarize all of the above, we can conclude that the oil-and-gas-bearing structure of the Dnipro-Donetsk Basin within its central rift part of mantle origin is a giant pathway of mantle hydrogen. Some of this hydrogen is consumed to form hydrocarbon fields and some of it degasses in the upper crust. Independent hydrogen fields can be formed there as well [Shestopalov et al., 2022]. Native aluminium is an indicator of these processes. The results achieved are also true for other basins, which contain native aluminium within the hydrocarbon fields.

Thus, native aluminum, as well as other native oxyphilic metals in sedimentary rocks of oil-and-gas bearing basins is a search marker of both hydrocarbon accumulations and the important role of deep geological hydrogen in the formation of these deposits and its possible accumulation in the most reliable traps.

Conclusions. 1. The process of native aluminum formation in the sedimentary rocks of the Dnipro-Donetsk Rift described above, as well as its findings in other basins indicates the typical character of this process for rift structures of hydrocarbon accumulation.

2. The oil-and-gas-bearing structure of Dnipro-Donetsk Rift is mantle origin and represents a giant source of mantle hydrogen.

3. Some of this hydrogen is consumed to form hydrocarbon accumulations, including known oil and gas deposits, and some of it degasses into the uppermost layers of the Earth's crust. Independent hydrogen fields can also form there, as was the case during the formation of the geological hydrogen field in Mali [Prinzhofer et al., 2018].

4. Native aluminumand other native oxyphilic metals in sedimentary rocks of oil-and-gas bearing rift basins are a search marker of both hydrocarbon accumulations and the important role of deep geological hydrogen in the formation of hydrocarbon deposits and its possible independent accumulation in the most reliable traps.

References

Avchenko, O.V., Chudnenko, K.V., & Alexandrov, I.A. (2009). *Basics of physical and chemical modeling of mineral systems*. Moscow: Nauka, 229 p. (in Russian).

Bajec, D., Grom, M., Lašič Jurković, D., Kostyniuk, A., Huš, M., Grilc, M., Likozar, B., & Pohar, A. (2020). A review of methane activation reactions by halogenation: catalysis, mechanism, kinetics, modeling, and reactors. *Processes, 8*(4), 443. https://doi.org/10.3390/pr8040443.

Bayrakov, V.V., Vishnevskiy, A.A., & Tishchenko, A.I. (2005). Native aluminum in terrigenous deposits of the Crimea. *Dopovidi NAN Ukrayiny,* (9), 102—106 (in Russian).

Berndt, M.E., Allen, D.E., & Seyfried, W.E. (1996). Reduction of CO_2 during serpentinization of olivine at 300 °C and 500 bar. *Geology, 24*(4), 351—354. https://doi.org/10.1130/0091-7613(1996)024<0351:ROCDSO>2.3.CO;2.

Bondarenko, V.I., Varlamov, G.B., & Volchin, I.A. (2005). From Fire and Water to Electricity. In I.N. Karp (Ed.), *Power Engineering: History, Present and Future* (Vol. 1). Kyiv (in Russian).

Chirvinskiy, P.N., & Cherkas, V.K. (1934). On the distribution of masses, pressures and densities in the Earth and its average chemical composition. *Trudy Mineralogicheskogo Muzeya AN SSSR,* (1), 103—119 (in Russian).

Chen, Z., Huang, C.-Y., Zhao, M., Yan, W., Chien, C.-W., Chen, M., Yang, H., Machiyama, H., & Lin, S. (2011). Characteristics and possible origin of native aluminum in cold seep sediments from the northeastern South China Sea. *Journal of Asian Earth Sciences, 40*(1), 363—370. https://doi.org/10.1016/j.jseaes.2010.06.006.

Dekov, V.M., Arnaudov, V., Munnik, F., Boycheva, T.B., & Fiore, S. (2009). Native aluminium: Does it exist? *American Mineralogist, 94*(8-9), 1283—1286. https://doi.org/10.2138/am.2009.3236.

Evans, B.W. (2004). The serpentine multisystem

revisited: chrysotileis metastable. *International Geology Review, 46*(6), 479—506. https://doi.org/10.2747/0020-6814.46.6.479.

Febrianto, S., Hastuti, E.P., & Sunaryo, G.R. (2019). Study on Pitting Corrosion of $AlMg_2$ in Solution Containing Chloride. *Journal of Physics: Conference Series, 1198*, 022061. https://doi.org/10.1088/1742-6596/1198/2/022061.

Foroulis, Z.A., & Thubrikar, M.J. (1975). A Contribution to the Study of the Critical Pitting Potential of Oxide Covered Aluminum in aqueous chloride solutions. *Materials and Corrosion, 26*(5), 350—355. https://doi.org/10.1002/maco.19750260505.

Frost, B.R., & Beard, J.S. (2007). On silica activity and serpentinization. *Journal of Petrology, 48*(7), 1351—1368. https://doi.org/10.1093/petrology/egm021.

González-Jiménez, J.M., Piña, R., Saunders, J.E., Plissarte, G., Marchesi, C., Padrón-Navarta, J.A., Ramón-Fernandez, M., Garrido, L.N.F., & Gervilla, F. (2021). Trace element fingerprints of Ni-Fe-S-As minerals in subduction channel serpentinites. *Lithos, 400-401*, 106432. https://doi.org/10.1016/j.lithos.2021.106432.

Gu, Y., Gammons, C.H., & Bloom, M. (1995). A one-term extrapolation method for estimating of aqueous reactions at elevated temperatures. *Geochimica et Cosmochimica Acta, 58*, 3545—3560. https://doi.org/10.1016/0016-7037(94)90149-X.

Halmann, M., Epstein, M., & Steinfeld, A. (2012). Carbothermic Reduction of Alumina by Natural Gas to Aluminium and Syngas: A Thermodynamic Study. *Mineral Processing and Extractive Metallurgy Review, 33*(5), 352—361. https://doi.org/10.1080/08827508.2011.601482.

Hasnan, N.S.N., Timmiati, S.N., Lim, K.L., Yaakob, Z., Hidayatul, N., Kamaruddin, N., & The, L.P. (2020). Recent developments in methane decomposition over heterogeneous catalysts: an overview. *Mater Renew Sustain Energy, 9*(8). https://doi.org/10.1007/s40243-020-00167-5.

Iyer, S.D., Mascarenhas-Pereira, M.B.L., & Nath, B.N. (2007). Native aluminium (spherules and particles) in the Central Indian Basin sediments: Implications on the occurrence of hydrothermal events. *Marine Geology, 240*(1-4), 177—184. https://doi.org/10.1016/j.margeo.2007.02.004.

Janecky, D.R., & Seyfried, W.E. (1986). Hydrothermal serpentinization of peridotite within the oceanic crust: Experimental investigations of mineralogy and major element chemistry. *Geochimica et Cosmochimica Acta, 50*(7), 1357—1378. https://doi.org/10.1016/0016-7037(86)90311-X.

Klein, F., Bach, W., Jons, N., McCollom, T., Moskowitz, B., & Berquo, T. (2009). Iron partitioning and hydrogen generation during serpentinization of abyssal peridotites from 15°N on the Mid-Atlantic Ridge. *Geochimica et Cosmochimica Acta, 73*(22), 6868—6893. https://doi.org/10.1016/j.gca.2009.08.021.

Koliabina, I.L., Sinitsyn, V.A., Shurpach, N.A., & Koliabina, D.A. (2009). Clay minerals in waste isolation technologies: modeling solubility of natural clays and verification of thermodynamic models for solid solutions of ylite and montmorillonite. *Heokhimiya ta rudoutvorennya,* (27), 124—127 (in Ukrainian).

Kolics, A., Besing, A.S., Baradlai, P., Haasch, R., Wieckowski, A. (2001). Effect of pH on Thickness and Ion Content of the Oxide Film on Aluminum in NaCl Media. *Journal of The Electrochemical Society, 148*(7), B251. https://doi.org/10.1149/1.1376118.

Kovalskiy, V.V., Oleynikov, O.B., & Mahotko, V.F. (1981). Native metals and intermetallic compounds in kimberlite rocks of Yakutia. In *Native mineral formation in the magmatic process: Abstracts of papers* (pp. 105—111). Yakutsk (in Russian).

Kulongoski, J.T., McMahon, P.B., Land, M., Wright, M.T., Johnson, T.A., & Landon, M.K. (2018). Origin of methane and sources of high concentrations in Los Angeles groundwater. *Journal of Geophysical Research: Biogeosciences, 123*, 818—831. https://doi.org/10.1002/2017JG004026.

Kupenko, V.I., & Osadchiy, E.G. (1981). Native aluminium in ores of Nikitovskoye ore deposit. In *Native mineral formation in the magmatic process: Abstracts of papers* (pp. 87—90) Yakutsk (in Russian).

Larin, N., Zgonnik, V., Rodina, S., Deville, E., Prinzhoferm, A., & Larin, V.N. (2015). Natural

Molecular Hydrogen Seepage Associated with Surficial, Rounded Depressions on the European Craton in Russia. *Natural Resources Research, 24*, 369—383. https://doi.org/10.1007/s11053-014-9257-5.

Leong, J.M., Ely, T., & Shock, E.L. (2021a). Decreasing extents of Archean serpentinization contributed to the rise of an oxidized atmosphere. *Nature Communications, 12*, 7341. https://doi.org/10.1038/s41467-021-27589-7.

Leong, J.M., Howells, A.H., Robinson, K.J., Cox, A., Debes, R.V., Fecteau, K., Prapaipong, P., & Shock, E.L. (2021b). Theoretical Predictions Versus Environmental Observations on Serpentinization Fluids: Lessons From the Samail Ophiolite in Oman. *Journal of Geophysical Research: Solid Earth*, *126*(4), e2020JB020756. https://doi.org/10.1029/2020JB020756.

Leong, J.M., Howells, A.H., Robinson, K.J., & Shock, E.L. (2018). Thermodynamic Predictions vs. Measured Fluid Chemistry: Lessons from Low-Temperature, Serpentinizing Fluids. *Ocean Worlds, Abstract 6025*. LPI Contribution No. 2085, Lunar and Planetary Institute, Houston.

Leong, J.M., & Shock, E.L. (2020). Thermodynamic constraints on the geochemistry of low-temperature, continental, serpentinization-generated fluids. *American Journal of Science, 320*(3), 185—235. https://doi.org/10.2475/03.2020.01.

Lepigov, G., Gulii, V., Lyzanets, A., & Tsyokha, O. (2011). Structure and gas content of the Shebelinsky deposit (in the light of the theory of abiogenic genesis of hydrocarbons). *Geologist of Ukraine,* (3-4), 48—52 (in Ukrainian).

Li, M., Xie, D.G., Ma, E., Li, J., Zhang, X.-X., Shan, Z.-W. (2017). Effect of hydrogen on the integrity of aluminium—oxide interface at elevated temperatures. *Nature Communications, 8*, 14564. https://doi.org/10.1038/ncomms14564.

Li, W., Cochell, T., & Manthiram, A. (2013). Activation of Aluminum as an Effective Reducing Agent by Pitting Corrosion for Wet-chemical Synthesis. *Scientific Reports, 3*, 1229. https://doi.org/10.1038/srep01229.

Lukin, A.E. (1997). *Lithogeodynamic factors of oil and gas accumulation in aulacogen basins*. Kiev: Naukova Dumka, 225 p. (in Russian).

Lukin, A.E. (2008). Native aluminum in oil and gas collectors. *Dopovidi NAN Ukrayiny,* (12), 100—107.

Lukin, A.E. (2004). On cross-formational fluid-conducting systems in oil-and-gas basins. *Geologichnyy Zhurnal,* (3), 34—45 (in Russian).

Lukin, A.E., Gafich, I.P., Goncharov, G.G., Makogon, V.V., & Prigarina, T.M. (2020). Hydrocarbon potential of subsoil in Ukraine and the principal ways of its development. *Mineral'ni resursy Ukrayiny,* (4), 28—38 (in Ukrainian).

Lukin, A., Savinykh, Yu., & Dontsov, V. (2007). On the native metals in oil-and-gas-bearing crystalline rocks of the White Tiger Field (Vietnam). *Geologist of Ukraine,* (2), 30—42.

Lukin, A.E., & Shestopalov, V.M. (2021). Tectono-magmatogene ring structures in zones of increased geodynamic instability as priority objects for exploration of hydrogen fields. *Geofizicheskiy Zhurnal, 43*(4), 3—41 (in Russian). https://doi.org/10.24028/gzh.v43i4.239953.

Marshintsev, V.K., Barashkov, Yu.P., & Leskova, N.V. (1981). Native elements in olivine from kimberlites. In *Native mineral formation in the magmatic process: Abstracts of papers* (pp. 103—105). Yakutsk (in Russian).

McCafferty, E. (2003). Sequence of steps in the pitting of aluminum by chloride ions. *Corrosion Science, 45*(7), 1421—1438. https://doi.org/10.1016/S0010-938X(02)00231-7.

McCollom, T.M., & Bach, W. (2009). Thermodynamic constraints on hydrogen generation during serpentinization of ultramafic rocks. *Geochimica et Cosmochimica Acta, 73(3)*, 856—875. https://doi.org/10.1016/j.gca.2008.10.032.

McCollom, T.M., Klein, F., Robbins, M., Moskowitz, B., Berquó, T.S., Jöns, N., Bach, W., & Templeton, A. (2016). Temperature trends for reaction rates, hydrogen generation, and partitioning of iron during experimental serpentinization of olivine. *Geochimica et Cosmochimica Acta*, 181(15), 175—200. https://doi.org/10.1016/j.gca.2016.03.002.

McCollom, T.M., Klein, F., Solheid, P., & Moskowitz, B. (2020). The effect of pH on rates of reaction and hydrogen generation during serpentinization. *Philosophical Transactions of the Royal Society A, Mathematical, Physical, and*

Engineering Sciences, 378(2165), 20180428. https://doi.org/10.1098/rsta.2018.0428.

Moody, J.B. (1976). Serpentinization: a review. *Lithos, 9*(2), 125—138. https://doi.org/10.1016/0024-4937(76)90030-X.

Naeini, M.F., Shariat, M.H., & Eizadjou, M. (2011). On the chloride-induced pitting of ultra fine grains 5052 aluminum alloy produced by accumulative roll bonding process. *Journal of Alloys and Compounds, 509*(14), 4696—4700. https://doi.org/10.1016/j.jallcom.2011.01.066.

Naumov, B.N., Ryzhenko, N.A., & Khodakovsky, G.B. (1971). Handbook of thermodynamic parameters. Moscow: Atomizdat, 240 p. (in Russian).

Nivin, V.A. (2016). Free hydrogen-hydrocarbon gases from the Lovozero loparite deposit (Kola Peninsula, NW Russia). *Applied Geochemistry, 74*, 44—55. https://doi.org/10.1016/j.apgeochem.2016.09.003.

Novgorodova, M.I. (1979). Findings of native aluminum in quartz veins. *Doklady AN SSSR, 248*(4), 965—968 (in Russian).

Novgorodova, M.I. (1983). *Native metals in hydrothermal ores*. Moscow: Nauka (in Russian).

Novgorodova, M.I., & Mamedov, Yu.G. (1996). Native aluminum from mud volcano on the Bulla Island (Caspian Sea). *Geologiya i poleznyye iskopayemyye,* (4), 339—349 (in Russian).

Oleynikov, B.V., Okrugin, A.V., & Leskova, N.V. (1978). Petrological significance of the occurrence of native aluminum in basites. *Doklady AN SSSR, 243*(1), 425—432 (in Russian).

Oleynikov, O.B., Vasiliev, Yu.R., & Makhotko, V.F. (1981). Native metals and natural alloys in picritic porphyrite from the northern part of Siberian Platform. In *Native mineral formation in the magmatic process: Abstracts of papers* (pp. 111—1141). Yakutsk (in Russian).

Olsen, E. (1963). Equilibrium calculations in the system Mg, Fe, Si,O, H, and Ni. *American Journal of Science, 261*, 943—956. https://doi.org/10.2475/ajs.261.10.943.

Othmer, D.F. (1974). *Method for producing aluminum metal directly from ore*. US Patent 3,793,003.

Paar, W.H., Ma, C., Topa, D., Culetto, F.J., Hammer, V.F.M., Guan, Y., & Braithwaite, R.S.W. (2019). Discovery of native aluminum on Variscan metagranitoids in Upper Carinthia, Austria: natural or anthropogenic origin? *Rendiconti Lincei. Scienze Fisiche e Naturali, 30*, 167—184. https://doi.org/10.1007/s12210-019-00760-5.

Palandri, J.L., & Reed, M.H. (2004). Geochemical models of metasomatism in ultramaflc systems: serpentinization, rodingitization, and sea floor carbonate chimney precipitation. *Geochimica et Cosmochimica Acta*, *68*(5), 1115—1133. https://doi.org/10.1016/j.gca.2003.08.006.

Peng, C., Liu, Y.-W., Guo, M.-X., Gu, T.-Z., Wang, C., Wang, Z.-Y., & Sun, C. (2022). Corrosion and pitting behavior of pure aluminum 1060 exposed to Nansha Islands tropical marine atmosphere. *Transactions of Nonferrous Metals Society of China, 32*(2), 448—460. https://doi.org/10.1016/S1003-6326(22)65806-0.

Peretti, A., Dubessy, J., Mullis, J.B., Frost, R., & Trommsdorff, V. (1992). Highly reducing conditions during Alpine metamorphism of the Malenco peridotite (Sondrio, northern Italy) indicated by mineral paragenesis and H^2 in fluid inclusions. *Contributions to Mineralogy and Petrology, 112*, 329—340. https://doi.org/10.1007/BF00310464.

Petrasch, J. (2002). *Thermal modeling of solar chemical reactors*. MSc. Thesis. ETH Zurich Swiss Federal Institute of Technology.

Porciúncula, C.B., Marcilio, N.R., Tessaro, I.C., & Gerchmann, M. (2012). Production of hydrogen in the reaction between aluminium and water in the presence of NaOH and KOH. *Brazilian Journal of Chemical Engineering, 29*(2), 337—48. https://doi.org/10.1590/S0104-66322012000200014.

Prinzhofer, A., Cissë, C.S.T., & Diallo, A.B. (2018). Discovery of a large accumulation of natural hydrogen in Bourakebougou (Mali). *International Journal of Hydrogen Energy, 43*(42), 19315—19326. https://doi.org/10.1016/j.ijhydene.2018.08.193.

Prinzhofer, A., Moretti, I., Francolin, J., Pacheco, C., d'Agostino, A., Werly, J., & Rupin, F. (2019). Natural hydrogen continuous emission from sedimentary basins: The example of a Brazilian H_2-emitting structure. *International Journal of Hydrogen Energy, 44*(12), 5676—5685.

https://doi.org/10.1016/j.ijhydene.2019.01.119.

Rains, R.K., & Kadlec, R.H. (1970). The reduction of Al2O3 to aluminium in a plasma. *Metallurgical Transactions, 1*(6), 1501—1506. https://doi.org/10.1007/BF02641992.

Saranchuk, V.I., Ilyashov, M.O., Oshovskiy, V.V., & Beletsky, V.S. (2008). *Basics of chemistry and physics of fossil fuels. (Textbook with the stamp of the Ministry of Higher Education).* Donetsk: Skhidnyy vydavnychyy dim, 638 p. (in Ukrainian).

Shestopalov, V.M., Koliabina, I.L., Ponomarenko, O.M., Lukin, A.E., & Rud, A.D. (2022). Thermodynamic assessment of the possibility of olivine interaction with deep-seated hydrogen. *International Journal of Hydrogen Energy, 47*(11), 7062—7071. https://doi.org/10.1016/j.ijhydene.2021.02.152.

Shnyukov, E.F., & Lukin, A.E. (2011). On native elements in various geoformations of the Crimea and adjacent regions. *Geologiya i poleznye iskopayemye Mirovogo okeana,* (2), 5—30 (in Russian).

Shestopalov, V.M., Lukin, A.Ye., Zgonnik, V.A., Makarenko, A.N., Larin, N.V., & Boguslavskiy, A.S. (2018). *Essays on the Earth Degassing*. Kiev, 632 p. (in Russian).

Shnyukov, E.F., Sobolevskiy, Yu.V., & Kutnyi, V.A. (1993). Genetic features of manganese-ore and phosphate mineralization in Barakol basin (Eastern Crimean Mountains). *Geologichnyy Zhurnal*, (1), 3—9 (in Russian).

Shock, E.L., & Helgeson, H.C. (1988). Calculation of the thermodynamic and transport properties of aqueous species at high pressures and temperatures: correlation algorithms for ionic species and equation of state predictions to 5 kb and 1000 °C. *Geochimica et Cosmochimica Acta, 52*, 2009—2036. https://doi.org/10.1016/0016-7037(88)90181-0.

Shock, E.L., Sassani, D.C., Willis, M., & Sverjensky, D.A. (1997). Inorganic species in geologic fluids: Correlations among standard molal thermodynamic properties of aqueous ions, hydroxide complexes. *Geochimica et Cosmochimica Acta, 61*, 907—950. https://doi.org/10.1016/S0016-7037(96)00339-0.

Shterenberg, L.E., Kuzmina, O.V., Laputina, I.P., & Tsepin, A.I. (1986). On finding of native aluminium associated with ZnO and $ZnCl_2$ in sediments, site 647 (northeastern Pacific). *Litologiya i poleznye iskopayemye,* (1), 137—140 (in Russian).

Shterenberg, L.E., & Vasilieva, G.L. (1979). Native metals and intermetallic compounds in sediments of the northeastern Pacific. *Litologiya i poleznye iskopayemye,* (2), 185—191 (in Russian).

Shterenberg, L.E., Voronin, B.I., & Stepanov, S.S. (1988). Partially oxidized native aluminium in sediments of the northeastern Pacific. *Byulleten' komissii po izucheniyu chetvertichnogo perioda, 57*, 110—116 (in Russian).

Silaev, V.I., Karpov, G.A., Anikin, L.P., Filippov, V.N., Petrovsky, V.A., Sukharev, A.E. & Simakova, Yu.S. (2017). The first discovery of natural duralumin. *Doklady Earth Sciences, 476*, 1048—1053. https://doi.org/10.1134/S1028334X17090082.

Sleep, N.H., Meibom, A., Fridrikssonm, Th., Coleman, R.G., & Bird, D.K. (2004). H_2-rich fluids from serpentinization: geochemical and biotic implications. *Proceedings of the National Academy of Sciences, 101*(35), 12818—12823. https://doi.org/10.1073/pnas.0405289101.

Smith, I.E. (1972). Hydrogen generation by means of the aluminium/water reaction. *Journal of Hydronautics, 6*(2), 106—109. https://doi.org/10.2514/3.48127.

Vijh, A. (1988). The pitting corrosion potentials of metals and surface alloys in relation to their solid state cohesion. *Materials Chemistry and Physics, 20*(4-5), 371—380. https://doi.org/10.1016/0254-0584(88)90075-2.

Wang, H.Z., Leung, D.Y.C., Leung, M.K.H., & Ni? M. (2009). A review on hydrogen production using aluminum and aluminum alloys. *Renewable and Sustainable Energy Reviews, 13*(4), 845—853, https://doi.org/10.1016/j.rser.2008.02.009.

Wetzel, L.R., & Shock, E.J. (2000). Distinguishing ultramafic from basalt-hosted submarine hydrothermal systems by comparing calculated vent fluid compositions. *Journal of Geophysical Research, 105*(B4), 8319—8340. https://doi.org/10.1029/1999JB900382.

Yu, S.Y., O'Grady, W.E., Ramaker, D.E., & Natishan, P.M. (2000). Chloride Ingress into Alu-

minum Prior to Pitting Corrosion an Investigation by XANES and XPS. *Journal of the Electrochemical Society, 147*, 2952. https://doi.org/10.1149/1.1393630.

Zucchetti, S., Mastrangelo, F., Rossetti, P., & Sandrone, R. (1988). Serpentinization and metamorphism: their relationships with metallogeny in some ophiolitic ultramafics from the Alps. *Zuffar' Days — Symposium in Honor of Piero Zuffardi. University of Cagliary, Cagliary (Italy), October 10—15* (Vol. 1, pp. 137—159).

Самородний алюміній як індикатор дегазації водню при формуванні родовищ вуглеводнів

О. Лукін*[1], *І. Колябіна*[2,3], *В. Шестопалов*[2], *О. Рудь*[3], *2023

[1]Інститут геологічних наук Національної академії наук України, Київ, Україна
[2]Радіоекологічний центр Національної академії наук України, Київ, Україна
[3]Інститут металофізики ім. Г.В. Курдюмова
Національної академії наук України, Київ, Україна

У статті розглянуто можливість транспортування самородного алюмінію з водневим флюїдом, його осадження та збереження в осадових породах, а також оцінювання умов, за яких це можливо. Зазначена проблема нині є дискусійною і розглядається у низці публікацій. Самородний алюміній знайдено в різних типах осадових порід нафтогазоносних басейнів. Зокрема, самородні алюмінієві сферули виявлені у доломітах Дніпровсько-Донецької западини. На прикладі цих знахідок показано, що необхідними умовами утворення і тривалого збереження самородного алюмінію є його міграція з потоком водню у верхні шари земної кори, формування *TP*-умов пароподібного стану води і утворення захисної плівки на поверхні самородного алюмінію. Описаний у статті процес утворення самородного алюмінію в осадових породах нафтогазових басейнів Дніпровсько-Донецького рифту, а також його виявлення в інших басейнах свідчить про типовий характер цього процесу для рифтових структур, де накопичуються вуглеводні. Припускається, що нафтогазоносна структура Дніпровсько-Донецького рифту має мантійне походження і є гігантським джерелом глибинного водню. Частина цього водню витрачається на формування скупчень вуглеводнів, у тому числі відомі родовища нафти та газу, а частина його дегазує у верхні шари земної кори. В результаті можуть утворюватися незалежні скупчення водню, як це було під час формування родовища геологічного водню в Малі. Показано, що наявність у флюїдах вуглеводнів не впливає на процеси, пов'язані з алюмінієм. Згідно з отриманими результатами значні потоки водню з мантії до верхніх горизонтів земної кори є значними. Наявність самородного алюмінію, як і інших самородних оксифільних металів в осадових породах нафтогазоносних басейнів, є пошуковим маркером як скупчень вуглеводнів, так і важливої ролі глибинного геологічного водню в утворенні цих скупчень і його можливого накопичення в надійних пастках.

Ключові слова: самородний алюміній, водневі флюїди, осадові породи.